

Supporting Information

“Honeycomb Catalytic Strategy” for Carbonylation Reaction Based on the Structural Evolution of Cobalt Species

**Peng Zhang ^{a,b,c}, Liying An ^{a,b,c}, Chunqiu Zhao ^b, Qiang Chang ^b, Fei Wang ^{a,b,*},
Chenghua Zhang ^{b,*}, Yulei Zhu ^{a,b}, Yong Yang ^{a,b}, Yongwang Li ^{a,b}**

^aState Key Laboratory of Coal Conversion, Institute of Coal Chemistry, Chinese Academy of Sciences, Taiyuan 030001, P. R. China

^bNational Energy Center for Coal to Liquids, Synfuels China Co., Ltd, Huairou District, Beijing 101400, P. R. China

^cUniversity of Chinese Academy of Sciences, No. 19A Yuquan Road, Beijing 100049, P. R. China

**E-mail: wangfei908@sxicc.ac.cn; zhangchh@sxicc.ac.cn*

Content

1. Computational Section

2. Supplementary Figures

Figure S1. H₂-TPR profiles of the supported cobalt catalysts.

Figure S2. XRD patterns of the supported cobalt catalysts.

Figure S3. XPS spectra of the supported cobalt catalysts.

Figure S4. TEM images of the supported cobalt catalysts.

Figure S5. (a) N₂ adsorption-desorption isotherms and (b) BJH desorption pore size distributions of the supported cobalt catalysts.

Figure S6. Catalytic performance of the Co/C catalyst on methoxycarbonylation of propylene oxide. Conversion (line) and selectivity (bar) as a function of (a) temperature, (b) pressure, and (c) time.

Figure S7. The yield of MHB and Co retention ratio for different catalysts after the reaction.

Figure S8. Photographs of supernatant of the Co/C catalyst under different post-treatment temperatures. (a) fresh reactants; (b) without post-treatment; (c) temperature, 75°C; (d) temperature, 190°C.

Figure S9. XRD patterns of the Co/C catalyst (a) fresh, (b) used, and (c) recycled 4 times through the “honey catalytic process”.

Figure S10. HRTEM and nanoparticles size distribution of the used Co/C catalyst.

3. Supplementary Tables

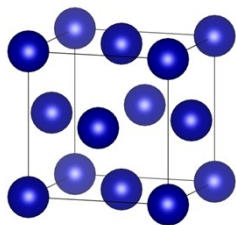
Table S1. BET specific surface area and cobalt loading amount of the supported catalyst.

Table S2. ICP-OES results of cobalt leaching from catalysts.

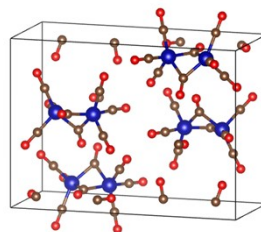
Table S3. Catalytic run of recycled Co/C catalyst in the methoxycarbonylation of propylene oxide.

1. Computational Section

In this section, we chose FCC-Co bulk and monoclinic $\text{Co}_2(\text{CO})_8$ crystals as calculated models, and crystal structures and unit cell parameters are shown in the table below.



FCC-Co



$\text{Co}_2(\text{CO})_8$

| | Space group | Lattice parameters (Å) | Angles (°) |
|----------------------------|------------------------|------------------------|----------------------------------|
| FCC-Co | Fm3m(225) | a=b=c=3.51 | $\alpha=\beta=\gamma=90$ |
| $\text{Co}_2(\text{CO})_8$ | P2 ₁ /m(11) | a=6.48 b=15.35 c=11.09 | $\alpha=\gamma=90$ $\beta=90.54$ |

2. Supplementary Figures

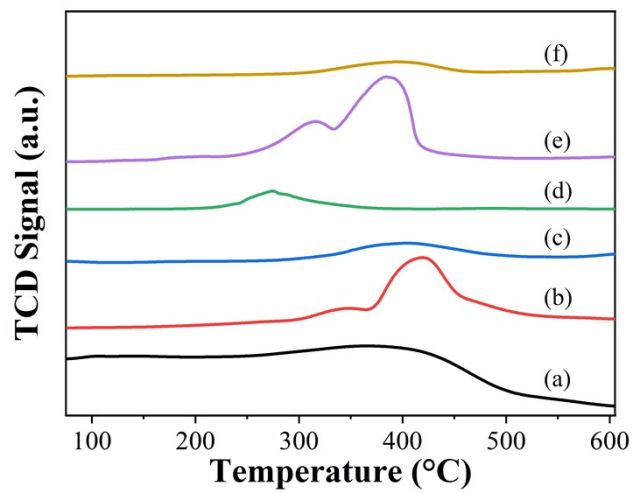


Figure S1. H₂-TPR profiles of the supported cobalt catalysts (a)Co/C, (b) Co/ γ -Al₂O₃, (c) Co/S1-Silicalite, (d) Co/SiO₂, (e) Co/TiO₂, and (f) Co/CeO₂.

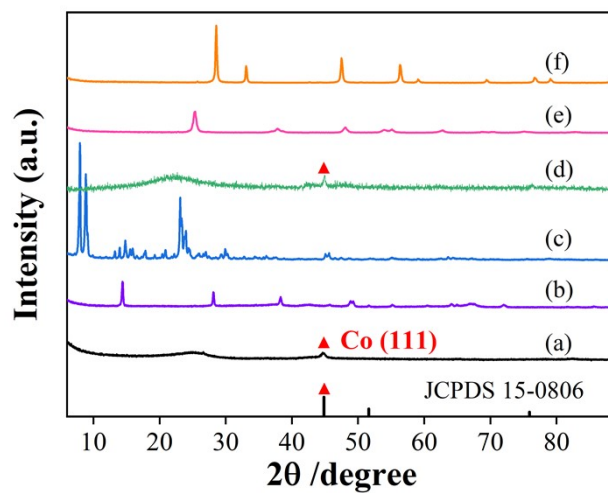


Figure S2. XRD patterns of the supported cobalt catalysts (a)Co/C, (b) Co/ γ -Al₂O₃, (c) Co/S1-Silicalite, (d) Co/SiO₂, (e) Co/TiO₂, and (f) Co/CeO₂.

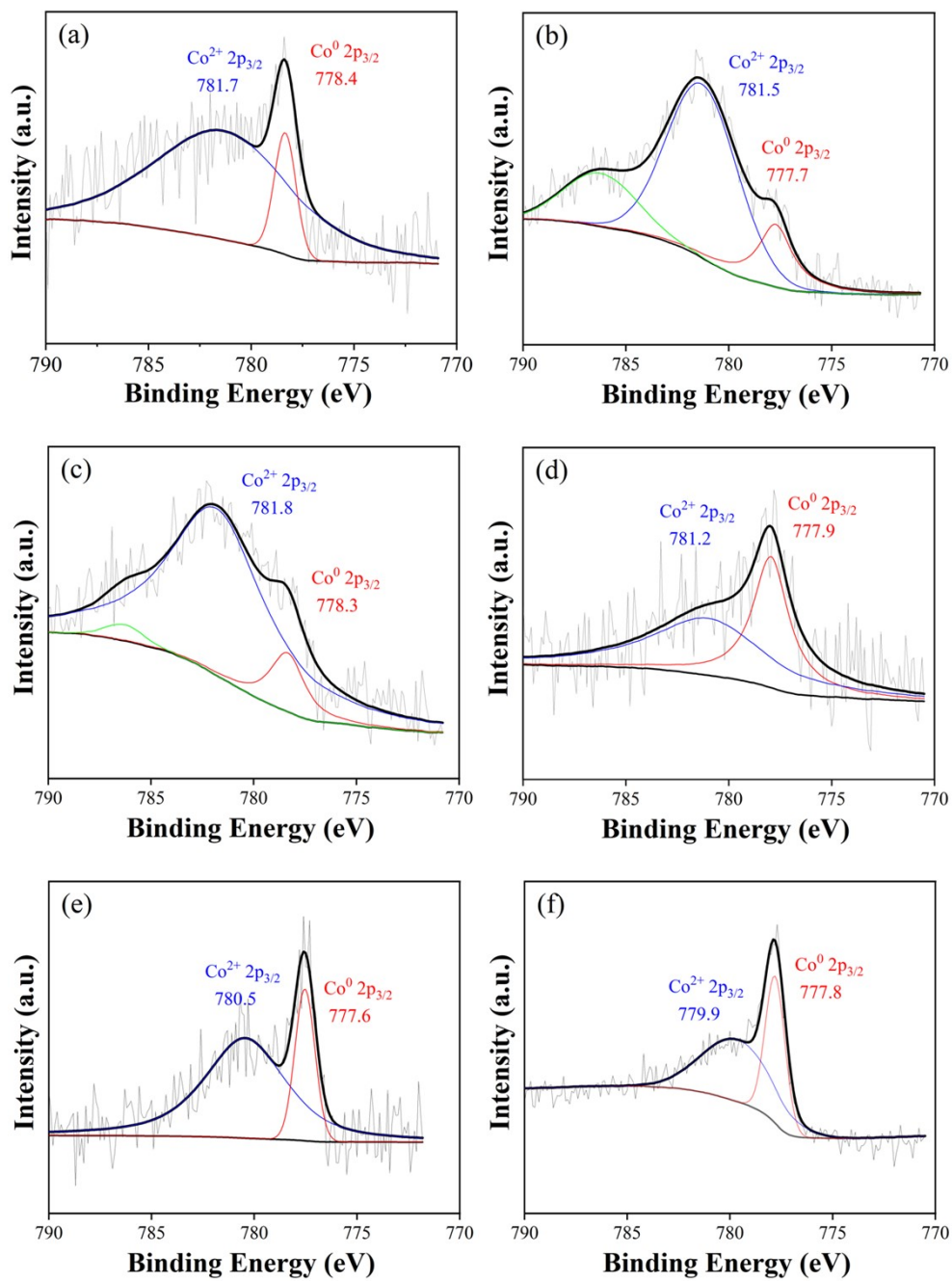


Figure S3. XPS spectra of the supported cobalt catalysts (a)Co/C, (b) Co/γ-Al₂O₃, (c) Co/S1-Silicalite, (d) Co/SiO₂, (e) Co/TiO₂, and (f) Co/CeO₂.

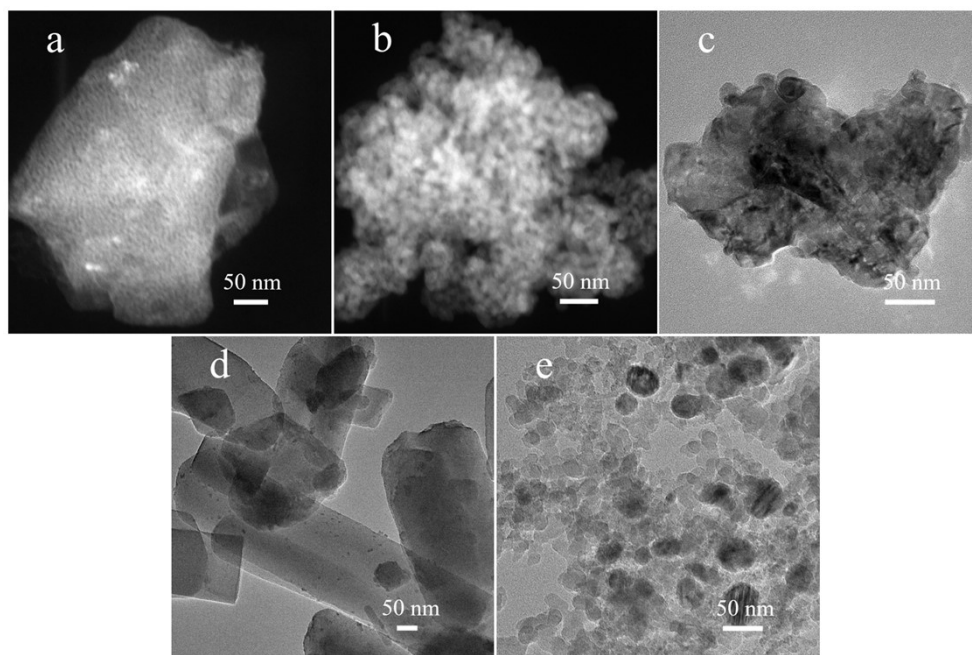


Figure S4. TEM images of the supported cobalt catalysts (a) γ - Al_2O_3 , (b) TiO_2 , (c) CeO_2 , (d) S1-Silicalite, and (e) SiO_2 .

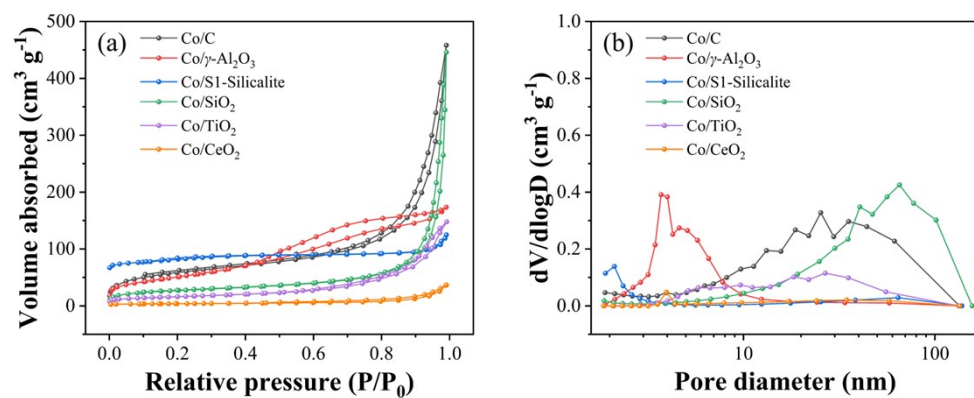


Figure S5. (a) N₂ adsorption-desorption isotherms and (b) BJH desorption pore size distributions of the supported cobalt catalysts.

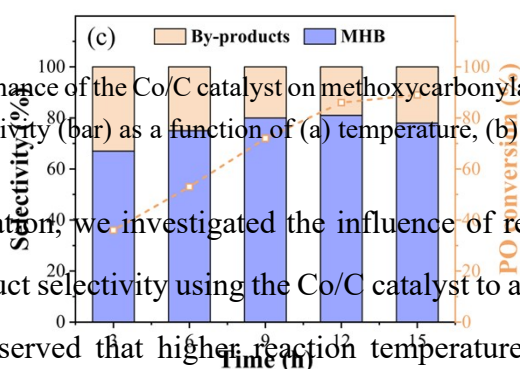
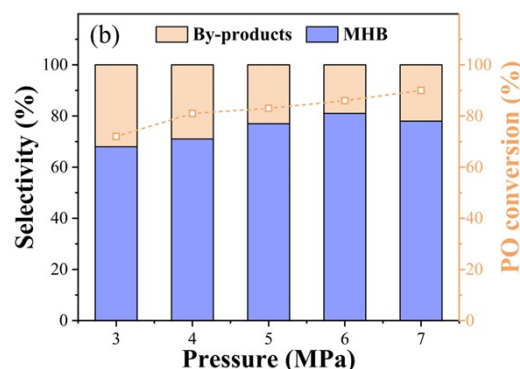
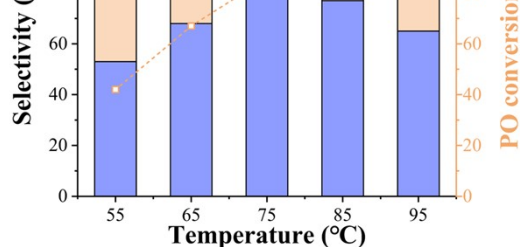


Figure S6. Catalytic performance of the Co/C catalyst on methoxycarbonylation of propylene oxide. Conversion (line) and selectivity (bar) as a function of (a) temperature, (b) pressure, and (c) time.

In the initial investigation, we investigated the influence of reaction conditions on PO conversion and product selectivity using the Co/C catalyst to attain optimal reaction performance. It was observed that higher reaction temperatures in this exothermic reaction were not conducive to achieving a high equilibrium yield and resulted in increased formation of by-products. While the PO conversion increased from 42% to 92% as the temperature rose from 55°C to 95°C, the highest yield of 70% MHB was obtained at 75°C. Hence, 75°C was selected as the optimal reaction temperature. Further optimization indicated that 6 MPa was sufficient, and a reaction time of 12 hours was advisable.

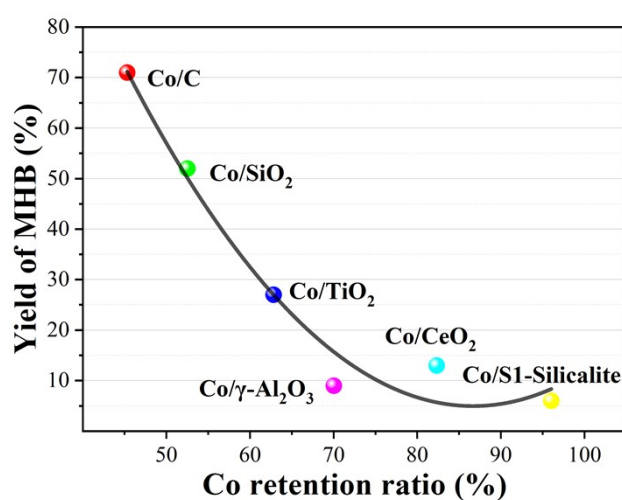


Figure S7. The yield of MHB and Co retention ratio for different catalysts after the reaction.

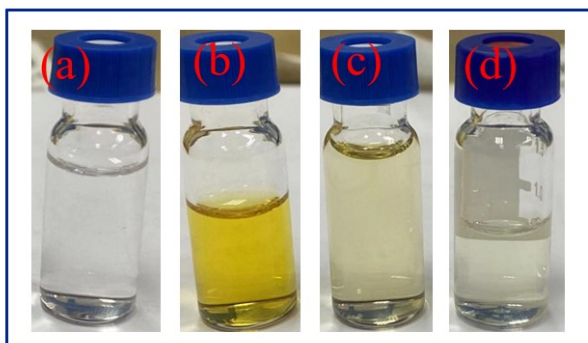


Figure S8. Photographs of supernatant of the Co/C catalyst under different post-treatment temperatures. (a) fresh reactants; (b) without post-treatment; (c) 75°C; (d) 190°C.

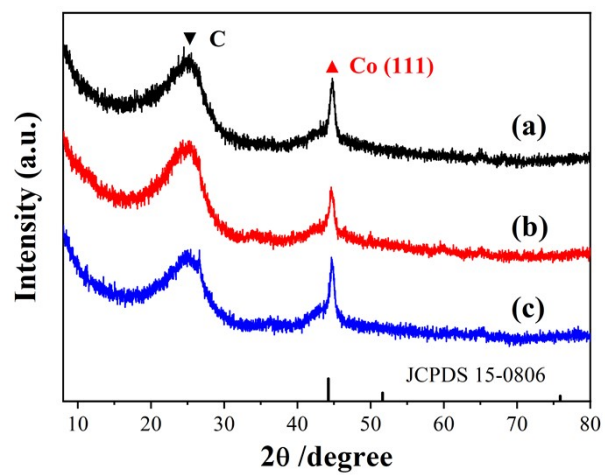


Figure S9. XRD patterns of the Co/C catalyst (a) fresh, (b) used, and (c) recycled 4 times through the “honey catalytic process”.

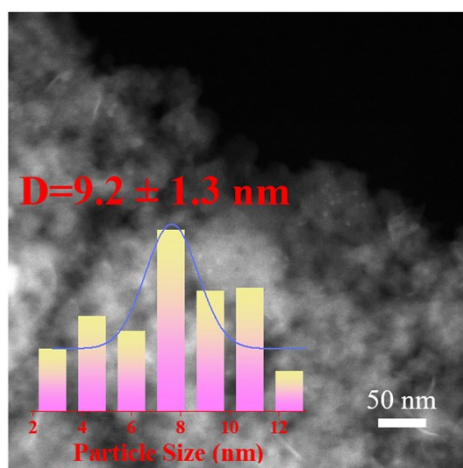


Figure S10. HRTEM and the cobalt nanoparticles size distribution of the used Co/C catalyst.

3. Supplementary Tables

Table S1. BET specific surface area and cobalt loading amount of the supported catalyst.

| Sample | Catalyst | Specific surface area (m ² /g) | Co loading (wt%) |
|--------|--|---|------------------|
| 1 | Co/C | 231.0 | 3.01 |
| 2 | Co/SiO ₂ | 97.6 | 3.04 |
| 3 | Co/TiO ₂ | 57.5 | 2.67 |
| 4 | Co/CeO ₂ | 13.3 | 2.72 |
| 5 | Co/ γ -Al ₂ O ₃ | 186.8 | 2.63 |
| 6 | Co/ S1-Silicalite | 278.6 | 2.84 |
| 7 | Co/C-1 | 217.9 | 10.40 |
| 8 | Co/C-2 | 201.7 | 20.79 |

Table S2. ICP-OES results of cobalt leaching from catalysts.

| Entry | Catalyst | Co content of supernatant ($\mu\text{g/g}$) ^a | Co retention ratio (%) ^a | Co content of supernatant ($\mu\text{g/g}$) ^b | Co retention ratio (%) ^b |
|-------|--|--|-------------------------------------|--|-------------------------------------|
| 1 | Co/C | 660.1 | 45.3 | 13.3 | 98.9 |
| 2 | Co/SiO ₂ | 573.4 | 52.5 | 9.5 | 99.2 |
| 3 | Co/TiO ₂ | 449.1 | 62.8 | 13.7 | 98.9 |
| 4 | Co/CeO ₂ | 213.6 | 82.3 | 15.4 | 98.7 |
| 5 | Co/ γ -Al ₂ O ₃ | 362.2 | 70.0 | 7.2 | 99.4 |
| 6 | Co/S1-Silicalite | 48.3 | 96.0 | 19.3 | 98.4 |
| 7 | Co/C-1 | 649.2 | 46.3 | 32.6 | 97.3 |
| 8 | Co/C-2 | 602.1 | 50.2 | 35.7 | 96.2 |

Standard reaction conditions: propylene oxide, 6 mmol; n[Co]/n[3-hydroxypyridine] = 1:3; methanol, 9 mL; initial pressure of CO, 6 MPa; reaction time, 12 hours; temperature, 75°C; catalyst, n[Co]/n[PO] = 1:40; stirring rate, 600 rpm.

^a Without post-treatment. ^b With post-treatment.

Post-treatment conditions: Venting CO slowly and charging N₂ with an initial pressure of 6 MPa; temperature, 190°C; time, 12 hours; stirring rate, 150 rpm.

Table S3. Catalytic run of recycled Co/C catalyst in the methoxycarbonylation of propylene oxide.

| Entry | Run | Conversion (%) | Selectivity (%) | Yield (%) | Co retention ratio (%) |
|-------|----------------|----------------|-----------------|-----------|------------------------|
| 1 | 1 ^a | 89 | 80 | 71 | 45.3 |
| 2 | 2 ^a | 53 | 65 | 34 | 23.7 |
| 3 | 3 ^a | 37 | 56 | 21 | 14.6 |
| 4 | 4 ^a | 24 | 13 | 3 | 8.9 |
| 5 | 1 ^b | 91 | 78 | 71 | 98.9 |
| 6 | 2 ^b | 86 | 76 | 65 | 97.1 |
| 7 | 3 ^b | 87 | 77 | 67 | 96.7 |
| 8 | 4 ^b | 84 | 75 | 63 | 95.2 |

Standard reaction conditions: propylene oxide, 6 mmol; n[Co]/n[3-hydroxypyridine] = 1:3; methanol, 9 mL; initial pressure of CO, 6 MPa; reaction time, 12 hours; temperature, 75°C; catalyst, n[Co]/n[PO] = 1:40; stirring rate, 600 rpm. Determined by gas chromatograph with diphenyl as an internal standard.

^a Without post-treatment. ^b With post-treatment.

Post-treatment conditions: Venting CO slowly and charging N₂ with an initial pressure of 6 MPa; temperature, 190°C; time, 12 hours; stirring rate, 150 rpm.